VIII International Conference on Fracture Mechanics of Concrete and Concrete Structures
FraMCoS-8
J.G.M. Van Mier, G. Ruiz, C. Andrade, R.C. Yu and X.X. Zhang (Eds)

A NEW INTERACTION-BASED NON LOCAL MODEL TO PREDICT DAMAGE AND FAILURE IN QUASI-BRITTLE MATERIALS

DAVID GRÉGOIRE*, LAURA B. ROJAS-SOLANO* AND GILLES PIJAUDIER-CABOT*

*Université de Pau et des Pays de l'Adour (UPPA)
Laboratoire des Fluides Complexes et leurs Réservoirs,
Allée du Parc Montaury, F64600 Anglet, France
e-mail: david.gregoire@univ-pau.fr, http://lfc.univ-pau.fr

Key words: Non local model, Non local interactions, Damage, Concrete failure, Quasi-brittle materials

Abstract. The purpose of this paper is to discuss a new approach to non-local interactions during failure in quasi-brittle materials. It focuses on the estimation of the non-local weight functions directly from interactions. The materials is modeled as an assembly of inclusions and the elastic interactions upon dilation of each inclusion are computed in a similar way to a classical Eshelby's problem. A new interaction-based weight function is then built from these interactions. This new interaction-based non local model is validated on simple 1D problems and its performances are compared with the classical integral-type nonlocal model.

1 INTRODUCTION

Classical failure constitutive models involve strain softening due to progressive cracking and a regularisation technique for avoiding spurious strain and damage localisation. Different approaches have been promoted in the literature such as integral-type non-local models (e.g. [1]), gradient damage formulations (e.g. [2]), cohesive cracks models (e.g. [3] with classical finite elements and e.g. [4] with extended finite elements), or strong discontinuity approaches (e.g. [5]). Such macroscale failure models have been applied on a wide range of problems, including the description of damage and failure in strain softening quasi-brittle materials [1], softening plasticity [6–8], creep [9] or composite degradation [10]. They may exhibit, however, some inconsistencies such as (*i*) incorrect crack initiation, ahead of the crack tip; (*ii*) propagating damage fronts after failure due to non-local averaging, (*iii*) incorrect shielding effect with non-zero non-local interactions across a crack surface; (*iv*) deficiencies at capturing spalling properly in dynamics, with spalls of zero thickness when the expected spall size is below the internal length of the model (see e.g. [11–14]). Moreover changing geometry, e.g. from tensile to bending loads or from unnotched to notched specimens, results generally in the loss of predictive capabilities of the macro-scale non-local models [15, 16]. On the contrary, it has been shown recently [15, 17] that meso-scale models gave good prospect in the prediction of failure and size effect for notched and unnotched concrete beams. Indeed meso-scale results have been compared to a new experimental database [16] consisting in 3 point bending failure tests for similar notched and unnotched concrete specimens of four different sizes but made from the same formulation. Not only the different peack loads for all geometries are recovered but also the failure softening phase is well predicted which is a more challenging issue. It means that the meso-scale

models intrinsically contain relevant information leading to a good description of the size effect, the boundary effect and the whole failure process.

At the macro-scale, the prediction of failure in quasi-brittle materials needs enhancement of existing non-local damage models and the way the non-locality is taken into account in the macro-scale models has to be redefined. Non-locality finds its origin in the interaction between material points undergoing damage in the course of failure [18, 19]. There are several mechanisms which should be considered when looking at the non-locality due to the interaction between damaged points : (i) an interaction exists if there is damage which produces this interaction. Assuming that damage corresponds to the growth of micro-cracks, this interaction grows with the size of the defect ; (ii) shielding effects are also expected : the interaction between two points located apart from a crack should not exist ; (iii) on free existing or evolving boundaries, and along the normal to these boundaries, non-local interactions should vanish as demonstrated in [20]. The internal length in the non-local model is the parameter inside the weight function that encompasses the non-locality and there is a consensus that this quantity may not be constant, but should depend on the geometry of the specimen or on the state of damage. Therefore enhanced non-local models accounting for a variation of the internal length have been proposed recently [13, 20, 21]. Proposals discussed in [13, 20] are considered on academic one-dimensional problems. Their implementation and extension to 2D or 3D problems are really not trivial as they involve the computation of path integrals, which are tedious in a finite element setting. The stress-based model in [21] is more tractable in 2D/3D computations but the evolution of non-locality is rather empirical.

The purpose of this paper is to discuss a new approach to non-local interactions during failure in quasi-brittle materials and to upscale the relevant information present from the meso-scale to the macro-scale. Therefore, the paper focuses on the estimation of the non-local weight function directly from interactions. The materials is modeled as an assembly of inclusions and the elastic interactions upon dilation of each inclusion are computed in a similar ways to a classical Eshelby's problem [22, 23]. A new interaction-based weight function is then built from these interactions. This new interaction-based non local model is first validated on simple 1D problems and its performances are compared with the classical integral-type nonlocal model.

2 A NEW INTERACTION-BASED NON-LOCAL MODEL

2.1 Non-locality in integral-type macro-scale models

In classical non-local models, such as the integral-type [1], the internal length is the parameter inside the weight function that encompasses the non-locality (see Eq. 1). Associated with a classical gaussian weight function, it set how and how far the interactions produce inside the materials. However, the main drawback of the formulation is that this parameter is constant whatever the geometry and the failure process. For instance, close to a boundary, the part of the nonlocal averaging domain that protrudes outside the boundary is classically chopped off [1]. Improved models can be found in the literature, with a different averaging process close to the boundary of the solid [12, 24] or with a varying internal length in the course of damage [13, 20, 21]. However, even if the internal length variations are based on micro-mechanical concepts, such as the crack growth interaction effect or the transfer of information through a damaged area, the final choice of the weigh function and thus the evolution of non-locality are rather empirical.

$$\begin{aligned} \overline{\varepsilon} &= \frac{1}{\Omega_r(x)} \int_\Omega \psi_0(x,\xi)\varepsilon(\xi)\mathrm{d}\xi \\ \psi_0(x,\xi) &= \exp\left(-\left(\frac{2||x-\xi||}{l_c}\right)^2\right) \\ \Omega_r(x) &= \int_\Omega \psi_0(x,\xi)\mathrm{d}\xi \end{aligned} \tag{1}$$

In Eq. 1, Ω is the volume of the structure, Ω_r is a characteristic volume introduced in such a way that the non-local operator does not affect the uniform field far away from the boundary, $\overline{\varepsilon}$ is the non-local strain, ψ_0 is a Gaussian weight function and l_c is the internal length of the non-local continuum which is related to the size of the fracture process zone.

2.2 Non-locality in meso-scale models

In meso-scale models, the non-locality is intrinsically included by representing the meso-structure of the materials (e.g. granular, matrix and interfaces in concrete). Therefore, the non-locality does not behave the same close to a boundary, close to a damaged area, at initiation or during the failure process. It has been shown recently that such models are able to capture challenging issues of quasi-brittle materials failure such as predicting the peak loads and even the whole softening load-displacement responses of notched and unnotched beams in three-point bending [15, 17]. In the following we aim at building a new interaction-based non-local weight function which will evolve intrinsically when damage occurs inside the materials.

2.3 A new interaction-based non-local weight function

The purpose of the paper is to discuss a new approach to non-local interactions during failure in quasi-brittle materials and to upscale the relevant information present from the meso-scale to the macro-scale. Therefore, we aim at estimating the non-local weight function ψ_0 presented in Eq. 1 directly from interactions.

Let us consider two material points (x, ξ) of a quasi-brittle structure and an infinitesimal strain perturbation locally produced in ξ. Considering the interaction between x and ξ consists in estimating the non-local contribution of the strain perturbation of ξ on x. This problem can be mathematically written as:

$$\begin{aligned} \overline{\varepsilon}_\xi(x) &= \int_\Omega \psi_x^{\text{int}}(u)\varepsilon_\xi^*(u)du \\ &= \int_\Omega \psi_x^{\text{int}}(u)\delta(\xi,u)\varepsilon^*(u)du \quad (2) \\ \delta(\xi,u) &= \begin{cases} 0 & \text{if} \quad u \neq \xi \\ 1 & \text{if} \quad u = \xi \end{cases} \quad (3) \end{aligned}$$

In Eq. 2, Ω is the volume of the structure, δ is the Dirac function, ε^* is a given strain field such as $\varepsilon_\xi^* = \delta\varepsilon^*$ represents the local strain perturbation centered in ξ, ψ_x^{int} is the interaction-based non-local weight function to reconstruct centered in x and $\overline{\varepsilon}_\xi(x)$ represents the non-local contribution of the strain perturbation of ξ on x.

Following Eq. 3, Eq. 2 can be rewritten as:

$$\overline{\varepsilon}_\xi(x) = \psi_x^{\text{int}}(\xi)\varepsilon^*(\xi) \quad (4)$$

Therefore the interaction-based non-local weight function ψ_x^{int}, centered on x, can be simply reconstructed by considering on each point ξ the measure of the non-local contribution seen by a point x when a perturbation is produced in ξ.

Practically, the interaction-based non-local weight function ψ_x^{int} is reconstructed using a finite element code *Cast3M*[1]. The strain perturbation is produced by a thermal expansion: $\varepsilon^* = \alpha\Delta T\ \mathbb{I}$. The thermal expansion is imposed on each integration points contained in a sphere centered in ξ (see Figure 1). The radius a of the sphere is a model parameter and is related to the size of the fracture process zone, i.e. to the maximum aggregate size. The measure of the non-local contribution is chosen equal to the Euclidean norm of the eigenstrains. Finally the interaction-based weight function writes:

$$\psi_x^{\text{int}}(\xi) = \sqrt{\sum_{i\in[\![1,3]\!]} |\epsilon_i^\xi(x)|^2} \quad (5)$$

In Eq. 5, $\epsilon_i^\xi(x)$ represents the value at point x of the ith-eigenstrain when a thermal expansion is imposed at point ξ.

[1] http://www-cast3m.cea.fr

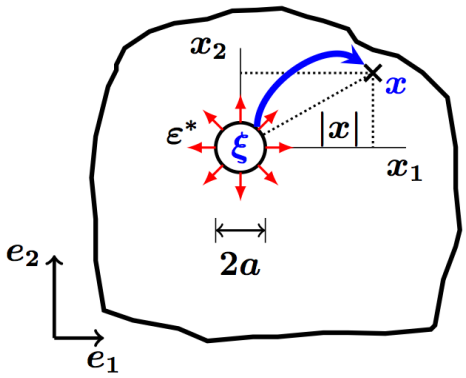

Figure 1: Non-local contribution seen by a point x when a perturbation is produced in ξ.

2.4 Eshelby-like problem

We aim here at validating the numerical implementation in the finite element code *Cast3M* of the interaction-based weight function reconstruction. Therefore we consider here a unique circular source of perturbation ξ in a large structure (see Fig. 2) and we estimate numerically the non-local contribution seen by the structure when a thermal expansion is produced in ξ.

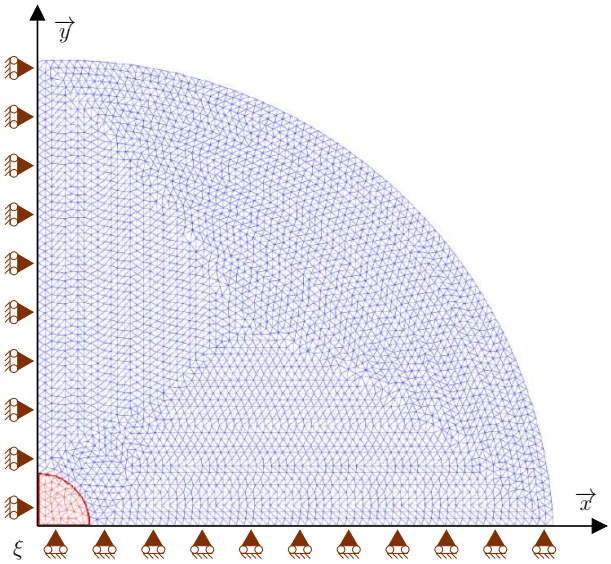

Figure 2: Eshelby-like problem

The numerical solution may be compared to the Eshelby-like solution of a circular inclusion[2] in a infinite medium [22, 23]. We will focus on the strain component along the Y-axis. From the Eshelby theory, for a circular inclusion of radius a, an initial dilation $\varepsilon^* = \alpha\Delta T\,\mathbb{I}$ (eigenstrain, i.e strain at 0-stress) and a Poisson ratio ν, the strain inside (ε^I) and outside (ε^E) the inclusion along the Y-axis are respectively given in Eq. 6 and 7 (see Eq. 15 and 16 in appendix for details).

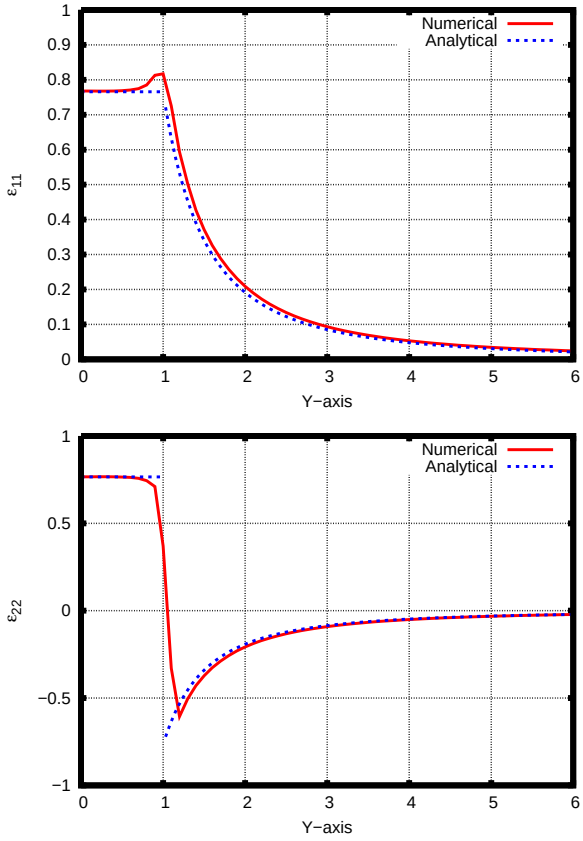

Figure 3: Comparison between the numerical results and the analytical Eshelby solution

$$\begin{aligned}\varepsilon^I &= \mathbb{S}^I\varepsilon^* = \mathbb{S}^I\alpha\Delta T\,\mathbb{I}\\ &= \alpha\Delta T\frac{1+\nu}{2(1-\nu)}\begin{bmatrix}1&0&0\\0&1&0\\0&0&0\end{bmatrix}\end{aligned} \tag{6}$$

$$\begin{aligned}\varepsilon^E &= \mathbb{S}^E\varepsilon^* = \mathbb{S}^E\alpha\Delta T\,\mathbb{I}\\ &= \alpha\Delta T\frac{a^2}{y^2}\frac{(1-\nu)}{2(1-\nu)}\begin{bmatrix}1&0&0\\0&-1&0\\0&0&0\end{bmatrix}\end{aligned} \tag{7}$$

Fig. 3 presents the comparison between the numerical results and the analytical Eshelby so-

[2] A 2D circular inclusion corresponds to a cylindrical inclusion in 3D

[3] $\alpha = 1K^{-1}$, $\Delta T = 1K$, $a = 1m$, $\nu = 0.21$

lution[3]. Both strains inside and outside the inclusion are recovered.

2.5 Final formulation

Damage is considered to be isotropic. Temperature and time-dependent effects are neglected. Therefore, the stress- strain relation is classically written as:

$$\sigma = (1-D)\mathbb{C} : \varepsilon \tag{8}$$

In Eq 8, $(\sigma, \varepsilon, \mathbb{C})$ are the stress, strain and stiffness tensors respectively, and D is the scalar damage variable which represents the material degradation ($D \in [0,1]$, $D = 0$ for a virgin material and $D = 1$ for a completely damage material).

Damage is a function of the amount of extension in the material, defined locally by the equivalent strain (Eq. 9), see Ref. [25].

$$\varepsilon_{eq} = \sqrt{\sum_{i \in [\![1,3]\!]} \langle \varepsilon_k \rangle_+^2} \tag{9}$$

In Eq 9, ε_k are the principal strains ($k = 1, 2, 3$) and $\langle \varepsilon_k \rangle_+$ their positive part.

The classical non-local integral formulation is modified by taking into account the new integration-based weight function presented in Eq. 5. Similarly to Eq. 1, a characteristic volume is introduced in such a way that the non-local operator does not affect the uniform field far away from the boundary when no damage occurs in the structure. Finally the non-local formulation writes:

$$\begin{aligned} \overline{\varepsilon}_{eq} &= \frac{1}{\Omega_r(x)} \int_\Omega \psi_x^{\text{int}}(\xi) \varepsilon_{eq}(\xi) \mathrm{d}\xi \\ \Omega_r(x) &= \int_\Omega \psi_x^0(\xi) \mathrm{d}\xi \end{aligned} \tag{10}$$

In Eq. 10, ψ_x^{int} is the new interaction-based weight function defined in Eq. 5 and ψ_x^0 represents the same function reconstructed when no damage occurs in the structure (typically at the beginning of the computation).

The evolution of damage (Eq. 11) is a function of the non-local equivalent strain (Eq.10) and it is governed by the Kuhn-Tucker loading-unloading condition (Eq. 11a).

$$\begin{aligned} \Gamma(\varepsilon, h) &= \overline{\varepsilon}_{eq}(\varepsilon) - h \quad , \quad \Gamma(\varepsilon, h) \leq 0 \quad , \\ \dot{h} \geq 0 \quad &, \quad \dot{h}\Gamma(\varepsilon, h) = 0 \\ h &= \max(\varepsilon_{D_0}, \max(\overline{\varepsilon}_{eq})) \end{aligned} \tag{11a}$$

$$\begin{aligned} D(\varepsilon_{eq}, x) &= \sum_{i \in \{t,c\}} \alpha_i [1 - (1 - A_i)\frac{\varepsilon_{D_0}}{\varepsilon_{eq}(x)} \\ &\quad - A_i \exp(-B_i(\varepsilon_{eq} - \varepsilon_{D_0}))] \\ \alpha_i &= \sum_{k \in [\![1,3]\!]} \left(\frac{\varepsilon_k^i \langle \varepsilon_k \rangle_+}{\varepsilon_{eq}^2} \right) \end{aligned} \tag{11b}$$

In Eq. 11a, Γ is the loading function which defines the limit of the elastic (reversible) domain, ε_{D_0} is the damage threshold, h is the history variable, the largest ever reached value of the non-local equivalent strain; in Eq. 11b, which defines the kinetics of damage growth, the damage variable is split into two parts to capture the differences of mechanical responses in tension $(i = t)$ and in compression $(i = c)$ as proposed by [25]. (α_t, α_c) are coefficients defined as functions of the principal values of the strain tensors $(\varepsilon^t, \varepsilon^c)$ due to positive and negative stresses, i.e. the strain tensors obtained according to Eq. 8 in which the positive (resp. negative) principal stresses are retained only. Note that in uniaxial tension $(\alpha_t = 1, \alpha_c = 0)$ and $(\alpha_t = 0, \alpha_c = 1)$ in uniaxial compression. (A_t, B_t, A_c, B_c) are model parameters.

Since the reconstruction process of the interaction-based weight function is kinematically driven by the successive thermal expansion imposed on each point of the structure, all boundary conditions are clamped during the reconstruction process in order to not perturb the actual kinematics fields on the boundary.

3 VALIDATION AND PERFORMANCES

3.1 Clamped bar in tension

There are several mechanisms which should be considered when looking at the non-locality due to the interaction between damaged points: (i) an interaction exists if there is damage which

produces this interaction. Assuming that damage corresponds to the growth of micro-cracks, this interaction grows with the size of the defect; (ii) shielding effects are also expected: the interaction between two points located apart from a crack should not exist; (iii) on free existing or evolving boundaries, and along the normal to these boundaries, non-local interactions should vanish as demonstrated in [20]. We propose here to test all these mechanisms on the simple problem of a clamped bar in tension (see Fig. 4). The response of the material is supposed to be purely elastic excepted in a damaged area located in the center of the bar. The structure is modeled as a succession of circular inclusions (radius a) which will be successively dilated in order to reconstruct the interaction-based non-local weight function. In order to study the response on the exact boundary, only half of an inclusion is used on both sides of the structure.

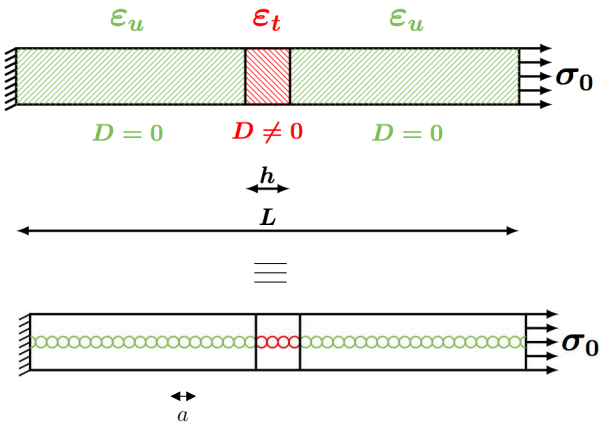

Figure 4: Simple problem of a clamped bar in tension.

Close to the left boundary, where no damage occurs, Fig. 5 shows that a local behavior is recovered when the size of the inclusions tends to zero. Therefore the non-local interactions vanish as proposed in [20].

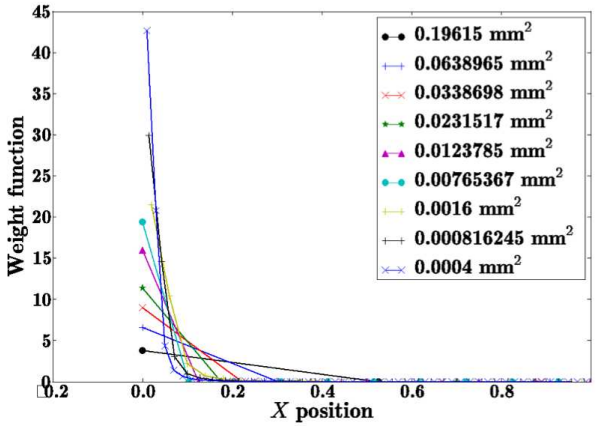

Figure 5: Local response close to a boundary for a decreasing size of the inclusion size.

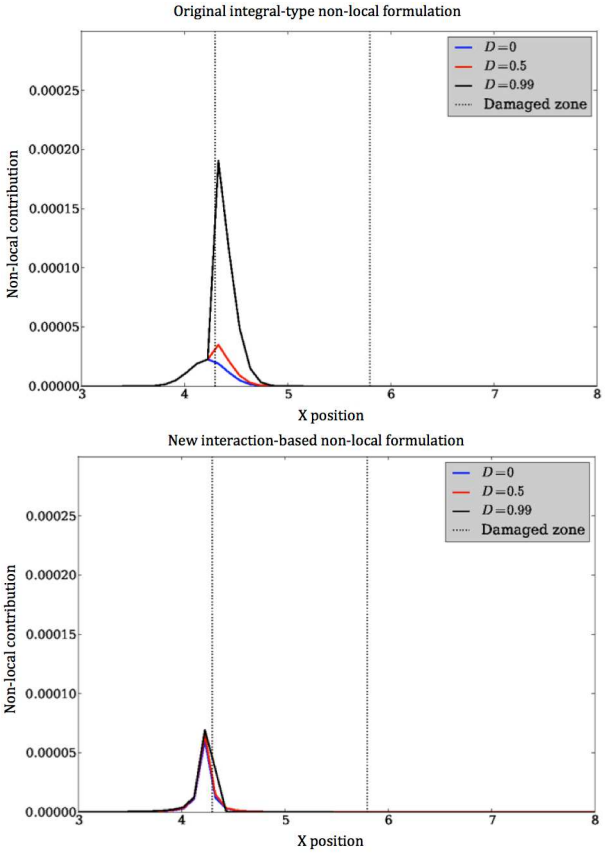

Figure 6: Response close to a damaged area.

When the inclusion stays inside the undamaged part but get close to a damaged area, Fig. 6 shows that a shielding effect is observed with the new formulation whereas the non-local contribution are higher inside the damaged area with the original formulation and the phenomenon increases when the damage increases.

If the size of the damage part decreases, this may lead to a transfer of information apart the damaged part with the original formulation whereas a perfect shielding effect is observed with the new one. The only restrictive condition is that the inclusion size stay smaller than the damaged area size otherwise some information may be transferred through the inclusion itself.

These first observations on a very simple example of a clamped bar in tension give some insight about the evolution of the size of the sphere containing the integration points where the thermal expansion is imposed to reconstruct the interaction-based weigh function. Indeed, this sphere has to decrease in size when it get close to a boundary in order to recover a local behavior. Moreover, this sphere has to decrease in size when the local damage increases to ensure an efficient shielding effect. Finally, we choose empirically the following rules:

$$a(x) \quad = \quad \min(a_0\sqrt{1-D(x)}, d(x)) \quad (12)$$

In Eq. 12, $a(x)$ represents the radius of the sphere containing the integration points where the thermal expansion is imposed to reconstruct the interaction-based weigh function, a_0 is a model parameter related to the maximum aggregate size, D is the local damage, d is the minimal distance from any boundary of the structure.

3.2 Dynamic failure of a rod

This example is used to test the relevance of the proposed model and its capabilities to describe progressive failure and complete failure. A bar is submitted at both extremities to constant strain waves, which propagate toward the center in the linear elastic regime (see Fig. 7 and Table 1). When the two waves meet at the center, the strain amplitude is doubled, the material enters the softening regime suddenly, and failure occurs. In all computations, the time step is chosen to be equal to the critical time step of the element size h, which is kept constant ($\Delta t_c = \frac{h}{\sqrt{E/\rho}}$, where E is the Young's modulus and ρ is the density).

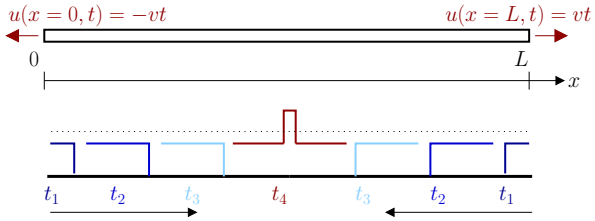

Figure 7: Dynamic failure of a rod: test description and time evolution of the strain amplitude repartition along the rod.

Table 1: Characteristics of the rod dynamic failure test

Parameter	L	v	E	ρ
Unit	cm	cms^{-1}	MPa	kgm^{-3}
Value	30	0.7	1	1

Parameter	lc / a_0	ε_{D_0}	α_t	A_t	B_t	α_c
Unit	cm	–	–	–	–	–
Value	4	1	1	1	2	0

In the course of damage, the crack opening displacement (COD) can be estimated using the method proposed by [26] and compared to an ideal crack opening profile obtained from a strong discontinuity analysis (single crack) (see Eq. 13). The comparison, e.g., the distance between the two profiles, indicates how close the strain and damage distributions are from those corresponding to a single crack surrounded by a fracture process zone.

$$\begin{aligned} [U](x) &= \frac{\overline{\varepsilon}(x)\Omega_r(x)}{\psi_0(x,x)} \\ \Delta(x) &= \frac{\int_\Omega ||\overline{\varepsilon}_{sd}(x,s) - \overline{\varepsilon}_{eq}(x)||ds}{\int_\Omega \overline{\varepsilon}_{eq}(s)ds} \\ \overline{\varepsilon}_{sd}(x,s) &= \frac{[U](x)\psi_0(x,s)}{\Omega_r(s)} \end{aligned} \quad (13)$$

In Eq. 13, $[U](x)$ is the COD computed at the point of coordinate x that corresponds to the location of the crack, $\Delta(x)$ represents the distance between an ideal opening profile obtained for a strong discontinuity (single crack at point of coordinate x), Ω_r is the representative volume, ψ_0 is the weight function, $\overline{\varepsilon}_{eq}$ is the nonlocal strain and $\overline{\varepsilon}_{sd}$ is a nonlocal strong discontinuity-based strain profile resulting from a crack located at coordinate x, e.g., the nonlocal strain

corresponding to a local strain described by a Dirac function. Details may be found in [13] based on [26].

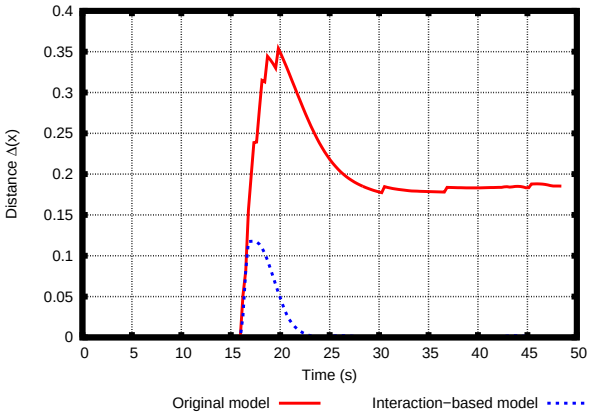

Figure 8: Dynamic failure of a rod: distance between the computed COD and an ideal opening profile obtained for a strong discontinuity versus time.

Figure 8 shows that the failure process is better described with the interaction-based model since the distance between its crack opening profile and the one corresponding to a strong discontinuity COD tends rapidly to zero.

At complete failure, the crack opening computed according to the above technique (see Eq. 13) should be independent of the element size. In a simple 1D setting, for instance, and assuming that the crack opening is smeared over the finite element that contains the discontinuous displacement at complete failure, the crack opening is equal to the strain distribution times the element size. Therefore, after complete failure, the strain in the cracked element should evolve in inverse proportion of the element size (for constant strain element) (see Eq. 14).

$$[U](x) \approx \varepsilon h = \text{constant} \qquad (14)$$

In Eq. 14, the COD $[U]$ has been smeared over the element that contains the crack (the other elements being completely unloaded at failure), ε is the strain in this element, and h is its size.

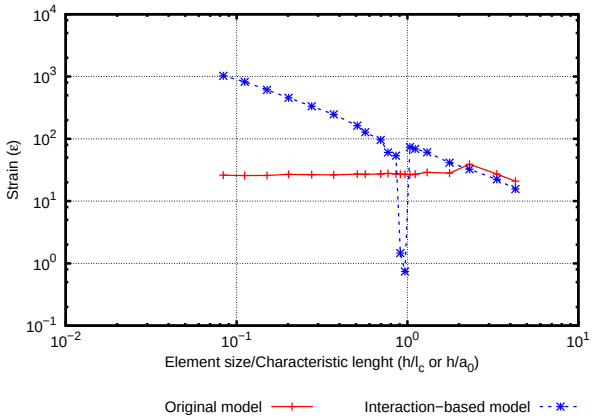

Figure 9: Dynamic failure of a rod: strain in the cracked element versus adimensional element size at complete failure.

Figure 9 shows that the complete failure is better described with the interaction-based model since the strain versus adimensional element size curve follows a linear trend in a logarithmic plot. Moreover the slope is coherent with the CMOD estimated at complete failure. Note that in the original model, the element size is dimensioned by the internal length l_c whereas in the new model, it is dimensioned by the characteristic length a_0. For the integration-based model, a peak discontinuity is observed when the element size is approximately equal to the characteristics length a_0. It means that several elements are needed inside the inclusion where is produced the perturbation to well reconstruct the interaction-based weight function.

3.3 Spalling test

A second 1D example is used to test the response of the new model close to a boundary. This 1D example consists of a spalling test presented by [12] based on a split Hopkinson pressure bar test primarily developed by [27] for material dynamic behavior characterization, but often adapted for dynamic fracture testing [28, 29]. A striker bar generates a square compressive wave that then propagates along the bar in the linear elastic regime. When this compressive wave reaches the free extremity of the bar, it is converted into a tensile wave and added to the incoming compressive wave (see Fig. 10 and Table 2). The resulting wave stays equal

to zero until the tensile one reaches a distance from the boundary equal to half the initial signal length. Failure is initiated at this point if the amplitude is greater than the tensile strength, generating a spall at a controlled distance from the boundary that depends on the initial compressive signal duration. For all numerical studies, the time step is chosen to be equal to the critical time step of the corresponding element size.

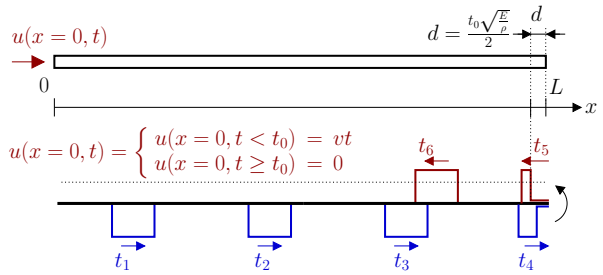

Figure 10: Spalling test: test description and time evolution of the strain amplitude repartition along the rod.

Table 2: Characteristics of the rod dynamic failure test

Parameter	L	t_0	v	E	ρ
Unit	cm	s	cms^{-1}	MPa	kgm^{-3}
Value	20	4	1.5	1	1

Parameter	lc / a_0	ε_{D_0}	α_t	A_t	B_t	α_c
Unit	cm	–	–	–	–	–
Value	4	1	1	1	2	0

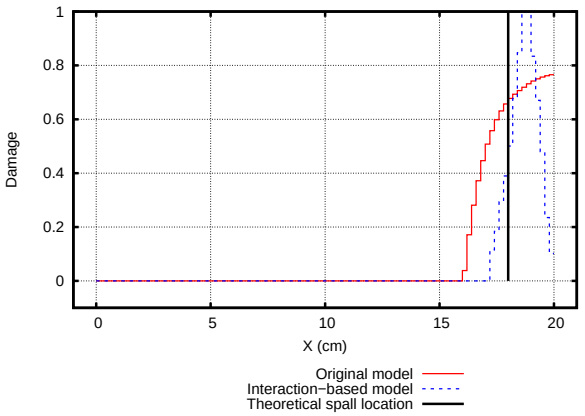

Figure 11: Spalling test: damage repartition along the bar after failure.

Figure 11 shows that the spalling failure is better described with the interaction-based model since the spall location is predicted inside the bar whereas the damage is maximum on the boundary with the original model.

4 CONCLUSION

A new interaction-based non-local formulation has been proposed. In this formulation, the materials is modeled as an assembly of inclusions and the elastic interactions upon dilation of each inclusion are computed in a similar ways to a classical Eshelby's problem. A new interaction-based weight function is then built from these interactions. This new interaction-based non local model has been first validated on simple 1D problems and its performances have been compared with the classical integral-type nonlocal model.

Different results have been presented in the paper:

- In the course of damage, the crack opening displacement has been estimated and the comparisons show that the failure process is better described with the new formulation. Indeed the crack opening profile is very close to an ideal opening profile obtained for a strong discontinuity.

- At complete failure, the crack opening should be independent of the element size. Therefore, after complete failure, the strain in the cracked element should evolve in inverse proportion of the element size, assuming that the crack opening is smeared over the finite element that contains the discontinuous displacement. It has been shown that for the new formulation, the strain versus element size curve follows a linear trend in a logarithmic plot. Moreover the slope is coherent with the CMOD estimated at complete failure.

- Close to a boundary, it has been shown that the spalling failure is better described

with the interaction-based model since the spall location is predicted inside the bar whereas the damage is maximum on the boundary with the original model.

Finally, it has been shown that this new interaction-based formulation fulfill several deficiencies of the classical integral-type nonlocal model and the formulation has to be implemented in 2D in order to test its performance on more challenging issues of quasi-brittle materials failure such as reproducing the peak loads and even the whole softening load-displacement responses of notched and unnotched beams in three-point experimental bending tests [16].

ACKNOWLEDGMENTS

Financial support from ERC advanced grant Failflow (27769) is gratefully acknowledged.

REFERENCES

[1] Pijaudier-Cabot G, Bazant ZP. Nonlocal Damage Theory. *Journal of Engineering Mechanics* 1987; **113**(10):1512–1533.

[2] Peerlings R, De Borst R, Brekelmans W, De Vree J, Spee I. Some observations on localisation in non-local and gradient damage models. *European Journal of Mechanics - A/Solids* 1996; **15**(6):937–953.

[3] Wells G, Sluys L. A new method for modelling cohesive cracks using finite elements. *International Journal for Numerical Methods in Engineering* 2001; **50**(12):2667–2682.

[4] Moës N, Belytschko T. Extended finite element method for cohesive crack growth. *Engineering Fracture Mechanics* 2002; **69**(7):813–833.

[5] Oliver J, Huespe A, Samaniego E, Chaves E. Continuum approach to the numerical simulation of material failure in concrete. *International Journal for Numerical and Analytical Methods in Geomechanics* 2004; **28**(7-8):609–632.

[6] Tvergaard V, Needleman A. Effects of nonlocal damage in porous plastic solids. *International Journal of Solids and Structures* 1995; **32**(8-9):1063–1077.

[7] Bažant Z, Jirásek M. Nonlocal integral formulations of plasticity and damage: survey of progress. *Journal of Engineering Mechanics* 2002; **128**:1119.

[8] Grassl P, Jirásek M. Plastic model with non-local damage applied to concrete. *International Journal for Numerical and Analytical Methods in Geomechanics* 2006; **30**(1):71–90.

[9] Saanouni K, Chaboche J, Lesne P. On the creep crack-growth prediction by a non local damage formulation. *European journal of mechanics. A. Solids* 1989; **8**(6):437–459.

[10] Germain N, Besson J, Feyel F. Composite layered materials: Anisotropic nonlocal damage models. *Computer Methods in Applied Mechanics and Engineering* 2007; **196**(41-44):4272–4282.

[11] Simone A, Askes H, Sluys L. Incorrect initiation and propagation of failure in non-local and gradient-enhanced media. *International journal of solids and structures* 2004; **41**(2):351–363.

[12] Krayani A, Pijaudier-Cabot G, Dufour F. Boundary effect on weight function in nonlocal damage model. *Engineering Fracture Mechanics* 2009; **76**(14):2217–2231.

[13] Grégoire D, Rojas-Solano L, Pijaudier-Cabot G. Continuum to discontinuum transition during failure in non-local damage models. *International Journal for Multiscale Computational Engineering* 2012; **10**(6):136.

[14] Jirasek M, Rolshoven S, Grassl P. Size effect on fracture energy induced by nonlocality. *International journal for numeri-*

cal and analytical methods in geomechanics 2004; **28**(7-8):653–670.

[15] Grégoire D, Grassl P, Rojas-Solano L, Pijaudier-Cabot G. Macro and mesoscale models to predict concrete failure and size effects. *Damage Mechanics of Cementitious Materials and Structures*, Pijaudier-Cabot G DFE (ed.). ISTE Ltd and John Wiley & Sons, Inc., 2012.

[16] Grégoire D, Rojas-Solano L, Pijaudier-Cabot G. Failure and size effect for notched and unnotched concrete beams. *International Journal for Numerical and Analytical Methods in Geomechanics* 2012, submitted; .

[17] Grassl P, Grégoire D, Solano L, Pijaudier-Cabot G. Meso-scale modelling of the size effect on the fracture process zone of concrete. *International Journal of Solids and Structures* 2012; **49**(13):1818–1827.

[18] Bažant Z. Nonlocal damage theory based on micromechanics of crack interactions. *Journal of engineering mechanics* 1994; **120**(3):593–617.

[19] Pijaudier-Cabot G, Berthaud Y. Effets des interactions dans l'endommagement d'un milieu fragile. formulation non locale. *Comptes rendus de l'Académie des sciences. Série 2, Mécanique, Physique, Chimie, Sciences de l'univers, Sciences de la Terre* 1990; **310**(12):1577–1582.

[20] Pijaudier-Cabot G, Dufour F. Non local damage model. *European Journal of Environmental and Civil Engineering* 2010; **14**(6-7):729–749.

[21] Giry C, Dufour F, Mazars J. Stress-based nonlocal damage model. *International Journal of Solids and Structures* 2011; **48**(25-26):3431–3443.

[22] Mura T. *Micromechanics of defects in solids*, vol. 3. Springer, 1987.

[23] Markenscoff X, Gupta A. *Collected Works of JD Eshelby : The Mechanics of Defects and Inhomogeneities*. Springer, 2006.

[24] Bažant Z, Le J, Hoover C. Nonlocal boundary layer (nbl) model: overcoming boundary condition problems in strength statistics and fracture analysis of quasibrittle materials. *Fracture Mechanics of Concrete and Concrete StructuresRecent Advances in Fracture Mechanics of Concrete (Proc., FraMCoS-7, 7th Int. Conf. held in Jeju, Korea, plenary lecture), B.-H. Oh, ed., publ. by Korea Concrete Institute, Seoul*, 2010; 135–143.

[25] Mazars J. A description of micro-and macroscale damage of concrete structures. *Engineering Fracture Mechanics* 1986; **25**(5-6):729–737.

[26] Dufour F, Pijaudier-cabot G, Choinska M, Huerta A. Extraction of a crack opening from a continuous approach using regularized damage models. *Computers and Concrete* 2008; **5**(4):375–388.

[27] Kolsky H. An investigation of the mechanical properties of material at a very high rate of loading. *Proceedings of the Physical Society* 1949; **B62**:676–700.

[28] Grégoire D, Maigre H, Réthoré J, Combescure A. Dynamic crack propagation under mixed-mode loading Comparison between experiments and X-FEM simulations. *International Journal of Solids and Structures* Oct 2007; **44**(20):6517–6534.

[29] Grégoire D, Maigre H, Combescure A. New experimental and numerical techniques to study the arrest and the restart of a crack under impact in transparent materials. *International Journal of Solids and Structures* Sep 2009; **46**(18-19):3480–3491.

APPENDIX
Analytical Eshelby solution of a circular inclusion in an infinite medium

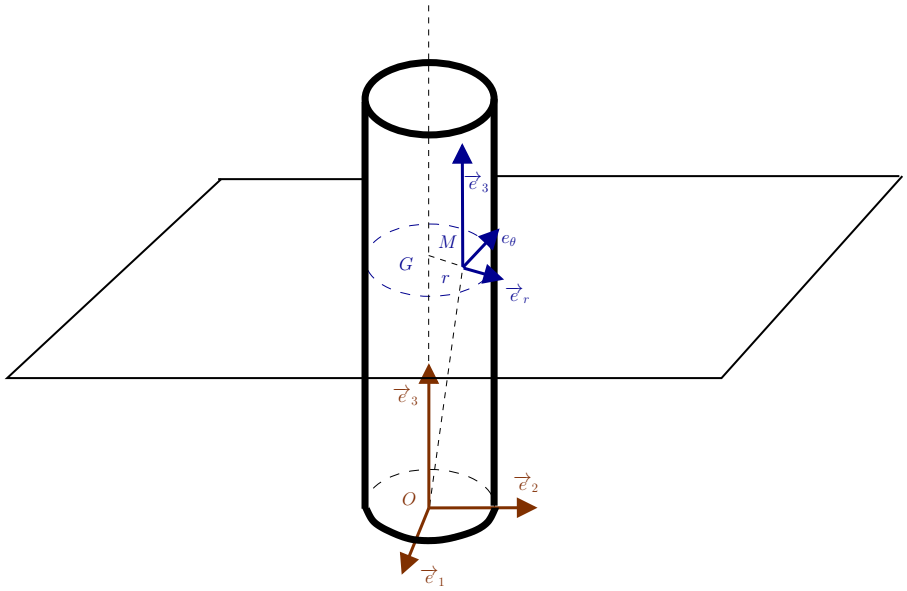

Figure 12: Eshelby-like problem of a circular inclusion in an infinite medium

From the Eshelby theory, for a circular inclusion of radius a, an initial dilation ε^* (eigenstrain, i.e strain at 0-stress) and a Poisson ratio ν, the strain inside (ε^I) and outside (ε^E) the inclusion are respectively given by:

$$\varepsilon^I_{ij} = \mathbb{S}^I_{ijmn}\varepsilon^*_{mn} \tag{15}$$

$$\forall\{i,j,m,n\} \in \{1,2\} \quad \begin{cases} S^I_{ijmn} = \dfrac{4\nu-1}{8(1-\nu)}\delta_{ijmn} + \dfrac{3-4\nu}{8(1-\nu)}(\delta_{imjn}+\delta_{injm}) \quad ; \\ S^I_{i3j3} = \dfrac{1}{4}\delta_{ij} \quad ; \quad S^I_{ij33} = \dfrac{\nu}{2(1-\nu)}\delta_{ij} \quad ; \\ S^I_{3jmn} = 0 \quad ; S^I_{33mn} = 0 \quad ; \quad S^I_{3j33} = 0 \quad ; \\ S^I_{ij3n} = 0 \quad ; \quad S^I_{333n} = 0 \quad ; \quad S^I_{3333} = 0 \end{cases}$$

$$\varepsilon^E_{ij} = \mathbb{S}^E_{ijmn}\varepsilon^*_{mn} \tag{16}$$

$$\forall\{i,j,m,n\} \in \{1,2\} \quad \begin{cases} S^E_{ijmn} = \dfrac{a^2}{8(1-\nu)x^4}\big[(4\nu x^2 - 2x^2 + a^2)\delta_{ij}\delta_{mn} \\ \quad + (-4\nu x^2 + 2x^2 + a^2)(\delta_{im}\delta_{jn} + \delta_{in}\delta_{jm}) \\ \quad - 4(2\nu x^2 - x^2 + a^2)\delta_{mn}x^0_i x^0_j + 4(x^2 - a^2)\delta_{ij}x^0_m x^0_n) \\ \quad + 4(\nu x^2 - a^2\left(\delta_{im}x^0_j x^0_n + \delta_{in}x^0_j x^0_m + \delta_{jm}x^0_i x^0_n + \delta_{jn}x^0_i x^0_m\right) \\ \quad + 8(3a^2 - 2x^2)x^0_i x^0_j x^0_m x^0_n\big] \\ S^E_{i3j3} = \dfrac{a^2}{4x^2}\left(\delta_{ij} - 2x^0_i x^0_j\right) \quad ; \quad S^E_{ij33} = \dfrac{\nu}{2(1-\nu)}\dfrac{a^2}{x^2}\left(\delta_{ij} - 2x^0_i x^0_j\right) \\ S^E_{3jmn} = 0 \quad ; \quad S^E_{33mn} = 0 \quad ; \quad S^E_{3j33} = 0 \quad ; \\ S^E_{ij3n} = 0 \quad ; \quad S^E_{333n} = 0 \quad ; \quad S^E_{3333} = 0 \\ \text{where } (r,\theta) \text{ are the polar coordinates:} \\ |x| = r,\ x^0_1 = cos\theta \text{ and } x^0_2 = sin\theta \end{cases}$$